PHYSICAL REVIEW B **70**, 094525 (2004)

Biaxial texture analysis of $YBa_2Cu_3O_7$-coated conductors by micro-Raman spectroscopy

J. C. González, N. Mestres, T. Puig, J. Gázquez, F. Sandiumenge, and X. Obradors
Institut de Ciència de Materials de Barcelona—CSIC, Campus UAB, E-08193, Bellatera, Spain

A. Usoskin, Ch. Jooss, and H. C. Freyhardt
Zentrum für Funktionwerkstoffe, 37073 Göttingen, Germany

R. Feenstra
Oak Ridge National Laboratory, Oak Ridge, Tennessee 37831-6057, USA

(Received 3 December 2003; revised manuscript received 6 April 2004; published 30 September 2004)

A quantitative determination of the degree of biaxial texture of $YBa_2Cu_3O_{7-\delta}$-coated conductors has been carried out by micro-Raman spectroscopy. The uniaxial texture is characterized by determining the *c*-axis grain fraction from the ratio between the intensity of $O(2,3)$-B_{1g} and $O(4)$-A_g modes. The degree of in-plane orientation is determined from the relative intensity modulation of the Raman phonon modes when samples are rotated around the axis perpendicular to the films. The biaxial texture parameter determined from Raman scattering has been modeled taking into account different grain misorientation distribution functions. The Raman results are compared with results of x-ray diffraction ϕ-scan measurements, and we demonstrate the relationship between the texture determination provided by both techniques. Additionally, the possibility of micro-Raman spectroscopy to perform local analysis allows one to characterize the texture uniformity of the superconducting films. The relationship between the biaxial texture determined by micro-Raman and the critical currents of coated conductors is further evidenced.

DOI: 10.1103/PhysRevB.70.094525 PACS number(s): 74.81.Bd, 78.30.−j, 74.72.−h

I. INTRODUCTION

Coated conductors are an interesting class of superconducting materials composed of $YBa_2Cu_3O_{7-\delta}$ (YBCO) biaxially textured grains deposited on a metallic substrate and separated by low-angle grain boundaries (GBs). High current density YBCO coatings have a high out-of-plane texture (*c*-axis oriented films) and a high inplane texture (*a*-*b* plane texture). These materials display very high critical current densities approaching those of epitaxial thin films and thus they have a very high potential for engineering applications like developing advanced power systems and high field magnets.[1] The grain boundaries of the YBCO layers are a direct reflection of the grain boundaries of the underlayer structures, i.e., textured Ni substrate.[2] The supercurrents flow through these GBs and therefore new physics related to current percolation through a network of grain boundaries is encountered. The local misorientation angle between the YBCO grains has been shown to be the main factor determining the critical currents.[3] Hence, the local texture study of the YBCO layer is of great relevance for understanding the properties of these materials.

Local analysis of the GBs of YBCO-coated conductors has been performed by transmission electron microscopy[4] and they have evidenced that the grain boundaries existing in high-quality samples are mainly [100]-tilt of less than 5–10°. In addition, electron backscattering diffraction has been envisaged as one of the best structural techniques to determine the local distribution of the grain-boundary structure in a quantitative and statistical manner.[5] However, the complexity of the method when applied to noncubic structures makes the direct characterization of the YBCO GBs rather difficult. Instead, the GBs of the underlayer cubic structures are systematically analyzed, i.e., the Ni textured substrate. In the case of YBCO layers deposited onto buffered yttria stabilized zirconia (YSZ) deposited on polycrystalline stainless steel substrates by ion beam assisted deposition (IBAD),[6] the difficulties are even larger since the small grain sizes of the underlayers ($\sim 0.5-1\ \mu m$) cannot be resolved by electron backscattering diffraction.

The potentiality of micro-Raman spectroscopy to determine the orientation of the crystal axes in YBCO films was first evidenced by Farrow *et al.*[7] The distinct selection rules for Raman scattering from the optical phonons of YBCO single crystals enable to determine the *c*-axis grain fraction in those films.[8,9]

Preliminary studies showed the capabilities of micro-Raman scattering to analyze the in-plane texture of YBCO films.[10–12] Thomsen *et al.*[11] investigated the degree of in-plane orientation of YBCO films consisting only of *c*-axis oriented crystals. Dieckmann *et al.*[12] extended the evaluation of the degree of epitaxy to the case where the superconductor films include *a*- and *c*-axis oriented crystallites. In these previous works, the samples were considered as a mixture of completely oriented and completely random crystals. A preliminary study determining the local degree of *c*-axis grain texture in YBCO IBAD-coated conductors was presented in Ref. 13.

In this paper, we present a thorough study of the biaxial texture of YBCO-coated conductors by micro-Raman spectroscopy. A specific methodology to characterize the local biaxial texture adapted to YBCO-coated conductors has been developed where, grain misoriented distribution functions have been taken into account. The relevance of the distribution function on the physical analysis of the material is con-

1098-0121/2004/70(9)/094525(8)/$22.50

clusive. A set of different coated conductors with distinct biaxial textures has been analyzed and the results have been compared to x-ray diffraction ϕ-scan measurements. The capability of micro-Raman to perform local analysis enables to extend the same methodology to local studies. Micro-Raman is, therefore, envisaged as a very useful technique to determine the local degree of c-axis fraction and the degree of in-plane orientation of YBCO-coated conductors.

II. EXPERIMENT

Seven samples grown by different methods and with different in-plane texture characterized by full width at half maximum (FWHM) x-ray ϕ-scan values expanding from 1.7° up to 17° have been analyzed in order to test the developed methodology and determine the degrees of c-axis grain fraction and in-plane orientation by micro-Raman. Six of them are YBCO-coated conductors, three YBCO IBAD and three YBCO rolling assisted biaxial textured substrates (RABiTs). The last sample, FILM-a, is a YBCO thin film of 250 nm grown on a $LaAlO_3$ single crystal by the trifluoroacetates metalorganic decomposition method[14] with a FWHM ϕ-scan of 1.7°.

A first IBAD sample, IBAD-a, was prepared by depositing a YBCO film by standard pulsed laser deposition (PLD) on a 20 nm CeO_2 buffered biaxially textured YSZ layer of 900 nm in thickness and deposited by IBAD on a polycrystalline YSZ substrate. It was 230 nm thick and had a ϕ-scan FWHM using the (102) reflection of 7.5°. The other two IBAD-coated conductors were prepared by depositing a 1.6-μm-thick $YBa_2Cu_3O_{7-x}$ film by a high rate PLD, on a nonmagnetic Ni-Cr stainless steel ribbon of 100 μm buffered with a biaxially textured YSZ layer of 900 nm in thickness and deposited by IBAD.[15] IBAD-b had a ϕ-scan FWHM value of 12.7° and IBAD-c had a ϕ-scan FWHM value of 17.2°.

The three RABiTs-coated conductors were prepared by growing a YBCO film by a BaF_2 *ex situ* process using evaporated precursors on a cube textured Ni tape microalloyed with 3% W with buffers of Ni (1 μm), Y_2O_3 (20 nm), YSZ (150 nm), and CeO_2 (20 nm).[16] RABiTs-a was 0.32 μm thick, RABiTs-b was 1 μm thick, and RABiTs-c was 2.4 μm thick. Their FWHM ϕ scans were 5.3°, 5.2°, and 6.6°, respectively.

In order to summarize the quality of the samples analyzed, we present in Fig. 1 the critical current density, J_c, at 77 K for the seven samples as a function of their ϕ-scan FWHM ($\Delta\phi$) using the (102) x-ray diffraction reflection. The critical current densities have been determined inductively as reported in Ref. 17. Notice that J_c follows the exponential decay with the misorientation angle in agreement with the literature,[3] which further evidences that the degree of biaxial texture is the main factor determining the critical currents in these granular materials.

Micro-Raman measurements were carried out using the 5145 Å line of an argon-ion laser at room temperature with a Jovin-Yvon T-64000 Raman spectrometer attached to an Olympus microscope and equipped with a liquid-nitrogen-cooled charge coupled device detector. Two focused laser spot sizes on the sample were used, ~1 or 10 μm in diameter depending on the analysis to be performed. The larger spot was used when an average measurement was to be performed and compared with x-ray data. The 1 μm spot was used for the local determination of film uniformity. The laser power onto the sample was kept below $\sim 12\ \mathrm{kW/cm^2}$ to avoid degradation on the films due to overheating of the proved volume. Raman spectra were recorded in backscattering geometry. The samples were mounted on the rotation X-Y stage of the microscope.

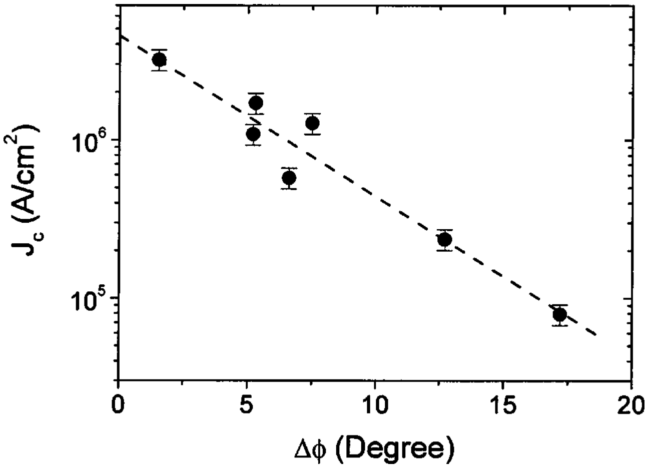

FIG. 1. Critical current densities, J_c; at 77 K for all the different coated conductors investigated in this work as a function of their ϕ-scan FWHM for the x-ray diffraction (102) reflection.

Two scattering geometries, *polarized* and *depolarized*, were used to obtain Raman spectra of the YBCO films. Spectra are called polarized when the directions of $\mathbf{e}_i$ and $\mathbf{e}_s$ are parallel to each other, and depolarized when they are perpendicular ($\mathbf{e}_i$ and $\mathbf{e}_s$ denote the directions of polarization of the incident and scattered light). A correction factor $K=1.9$ was applied to the spectra measured in polarized configuration, to correct for the efficiency of the collecting optics and spectrometer in this configuration.

III. RESULTS AND DISCUSSION

A. Uniaxial texture

Two phonon peaks in the Raman spectrum have been used in the structural characterization of YBCO thin films. The peak at 340 cm^{-1} (B_{1g}-like) associated with the out-of-phase vibration of the O(2)-O(3) oxygen atoms in the CuO_2 planes, and the peak at 500 cm^{-1}, an A_g mode involving the apical oxygen atoms O(4) vibrations.[18,19] By using the integrated intensities of these two Raman modes for different sample geometries we have developed a methodology to determine the biaxial texture of coated conductors taking into account the distribution function of the misoriented grains. However, we have first determined their out-of-plane orientation (uniaxial texture). In this case, we have applied the same principles reported in Ref. 12 to determine the uniaxial texture of coated conductors, and specifically (as explained in the next section) we have determined the local uniaxial texture to estimate the size and distribution of the *a*- and *c*-oriented crystals.

In the nearly tetragonal symmetry, the Raman tensors $\mathbf{R}_{B_{1g}}$ and $\mathbf{R}_{A_g}$ corresponding to the O(2)-O(3) and O(4) modes have the forms

$$\mathbf{R}_{B_{1g}} = \begin{pmatrix} x_{B_{1g}} & 0 & 0 \\ 0 & -y_{B_{1g}} & 0 \\ 0 & 0 & 0 \end{pmatrix},$$

$$\mathbf{R}_{A_g} = \begin{pmatrix} x_{A_g} & 0 & 0 \\ 0 & y_{A_g} & 0 \\ 0 & 0 & z_{A_g} \end{pmatrix}. \tag{1}$$

For our calculations we have used the values of the Raman tensor elements taken from Ref. 12, and they are: $x_{A_g}^2 = y_{A_g}^2 = 2$, $z_{A_g}^2 = 100$, $x_{B_{1g}}^2 = y_{B_{1g}}^2 = 8.5$.

Remember that the Raman intensity for a given phonon mode is proportional to

$$I \propto |\mathbf{e}_s \cdot \mathbf{R} \cdot \mathbf{e}_i|^2 \tag{2}$$

where $\mathbf{e}_i$ and $\mathbf{e}_s$ denote the polarization directions of incident and scattered light, respectively, and $\mathbf{R}$ is the corresponding Raman tensor for the vibration mode being considered.

According to the Raman scattering selection rules and with the Raman tensor elements given earlier, the O(2,3)-$\boldsymbol{B}_{1g}$ mode should be strong for grains which *c* axis is oriented perpendicular to the substrate plane (*c*-axis oriented grains), while the O(4)-A_g mode should appear weak; the opposite is expected for *a*-axis oriented grains. Therefore, the determination of the *c*-axis fraction is a measure of the uniaxial texture quality.

Figure 2 shows typical Raman spectra of two different YBCO IBAD-coated conductors with polarized and depolarized scattering geometries. Figure 2(a) shows the typical Raman spectra of a sample with a large fraction of *c*-axis oriented grains. On the contrary, the strong intensity of the O(4)-A_g phonon mode of Fig. 2(b) is an indication of a film with a large fraction of *a*-axis oriented grains.

In order to quantify the fraction of *c*- and *a*-axis oriented grains in a film, we consider that the intensity of the Raman signal is the sum of the intensity I_c of the *c*-axis oriented part and I_a of the *a*-axis oriented part of the film[12]

$$I = \delta I_c + (1-\delta) I_a. \tag{3}$$

According to this equation, the parameter δ is close to unity for *c*-axis oriented films and close to zero for *a*-axis oriented films.

The *c*-axis oriented grain fraction, δ, can be then calculated from the Raman intensity ratio

$$r = \frac{I_{B_{1g}}}{I_{A_g}}, \tag{4}$$

and the Raman tensors element values of the O(2,3)-B_{1g} and O(4)-Ag modes, using the equation

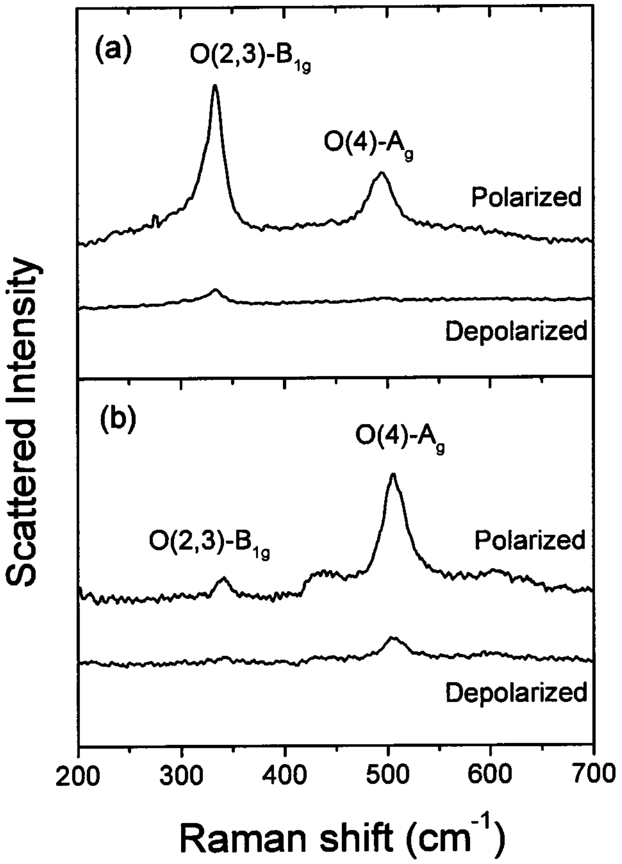

FIG. 2. Polarized and depolarized Raman spectra for two YBCO IBAD-coated conductors with different fraction of *c*-axis oriented grains, δ. (a) $\delta = 0.92 \pm 0.05$, (b) $\delta = 0.03 \pm 0.05$.

$$\delta = \frac{r(z_{A_g}^2 + x_{A_g}^2) - x_{B_{1g}}^2}{r(z_{A_g}^2 - x_{A_g}^2) + x_{B_{1g}}^2}. \tag{5}$$

In Eq. (4), the total intensity, for each mode, is the sum of the integrated intensities in the polarized and depolarized spectra. For the total intensity $I_{B_{1g}}$ of the O(2,3) mode, we determined the integrated intensities by fitting the peak with a Fano profile,[19] and for the total intensity I_{A_g} of the O(4) mode, by fitting the peak with a Lorentz profile. The δ values extracted from the Raman measurements for the two samples displayed in Figs. 2(a) and 2(b) are $\delta = 0.92 \pm 0.05$ and 0.03 ± 0.05, respectively.

This simple model does not include any distribution of grain tilting with respect to perfect on-axis orientation identified in x-ray diffraction as the FWHM of the ω scan ($\Delta\omega$). However, all the samples investigated in this work show $\Delta\omega$ always below 5°. We have estimate an error value in the δ-parameter determination below 3% for neglecting the grain tilt for samples with $\Delta\omega < 5°$.

Figure 3 shows the values for δ extracted from the Raman measurements as a function of the FWHM ϕ-scan x-ray diffraction data of the (102) reflection for all the different coated conductors investigated in this work. Notice that all seven samples analyzed have δ values above 0.9 indicating that less than a 10% of the sample had *a*-axis grain growth. We demonstrate that there should not exist any correlation

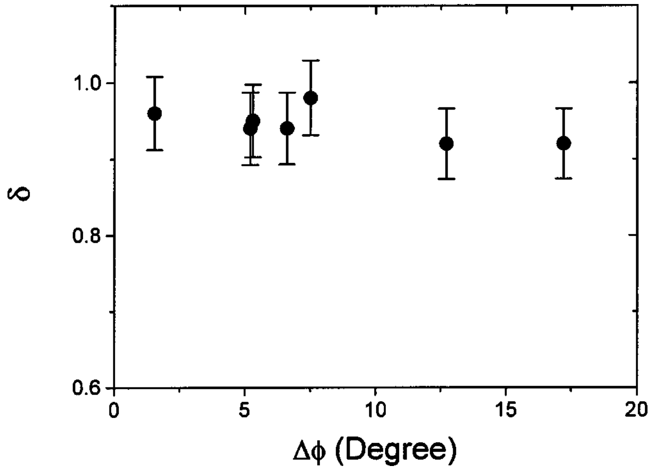

FIG. 3. Fraction of *c*-axis oriented crystals, δ, extracted from the Raman measurements as a function of the FWHM ϕ-scan x-ray diffraction data (102) reflection for all the different coated conductors investigated in this work.

between the degree of *c*-axis grain fraction and the distribution of in-plane grain orientations.

The δ results, obtained by averaging five different 10 μm laser spot Raman measurements, were compared to the *c*-axis grain fraction deduced from x-ray diffraction patterns recorded in the Bragg-Brentano geometry taking into account the structure factor of the Bragg reflections.[13,20] A fairly good agreement within a 5% was obtained between the two methods. This demonstrates that micro-Raman spectroscopy is a very suitable technique to determine the *c*-axis grain fraction of coated conductor samples. In the following section we will apply this methodology to perform local line scans on the investigated samples.

Moreover, since the visible light used in micro-Raman scattering has a penetration depth of about 80 nm in YBCO,[21] these analysis may be useful to determine depth profiles of *c*-axis grain fraction in thick coated conductors (>1 μm) which are unable to be acquired by x-ray diffraction.

B. Local evaluation of uniaxial texture

Micro-Raman scattering offers the unique possibility to perform Raman-microprobe scans and to test the structure of the films at a microscopic level. We have tested this capability in some of the coated conductor samples analyzed in this work, both concerning the degree of *c*-axis grain fraction and the degree of in-plane orientation (as it will be described in Sec. III D).

Figures 4(a) and 4(b) show line scans of 1 μm resolution performed to the samples RABiT-c and IBAD-b, respectively. These measurements have enabled to determine the degree of *c*-axis fraction in each measured position following the model described in Sec. III A and, therefore, we have evaluated if the YBCO layers have long range order over distances much larger than the diameter of the focused laser beam. For this reason the laser spot used was ~ 1 μm. Notice that sample RABiT-c is a perfect *c*-crystal sample within the experimental error [see Fig. 4(a)], whereas IBAD-b is a dominant *c*-crystal sample with the appearance of some *a* crystals, of ~ 2 μm size, randomly distributed [see Fig. 4(b)]. We conclude that micro-Raman spectroscopy is a very suitable technique to determine the uniformity of the uniaxial texture of coated conductors, to identify the appearance of *a* crystals even in high *c*-crystal fraction samples and to estimate their size and distribution.

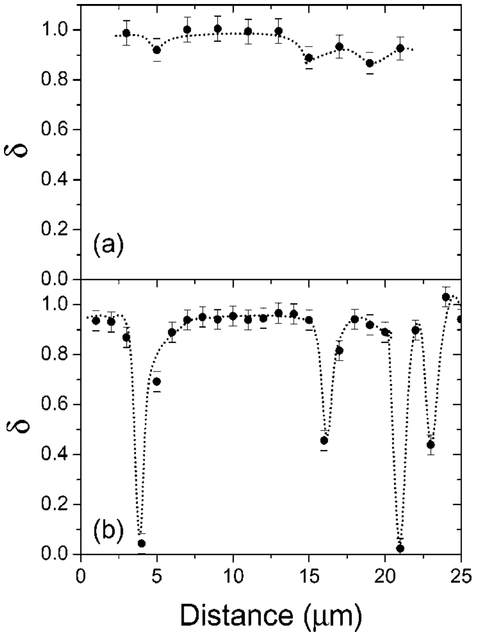

FIG. 4. δ values obtained along line scans measured with 1 μm spatial resolution on samples RABiT-c (a), and IBAD-b (b).

C. In-plane orientation

The intensity of the Raman signal in crystalline YBCO strongly depends on the scattering geometry and the relative orientation between the sample and the polarization direction of the incident and scattered light. This makes it possible to find the directions of the crystallographic axes of the film crystals in relation to the substrate axes, i.e., the degree of in-plane orientation. By rotating the angle between the crystallographic axes of the film crystals and the polarization direction of the incident laser, the scattered intensity for O(2,3)-B_{1g} and O(4)-A_g modes in polarized and depolarized geometries oscillates generating an angular modulated function. We are interested in developing a simple and truthful method for easier and practical characterization of in-plane-texture of YBCO-coated conductors which in addition takes into account the distribution of misoriented grains.

We are dealing with textured coatings characterized by a narrow grain misorientation distribution, directly related to the FWHM of the ϕ-scan XRD spectra $(1.7° < \Delta\phi < 17°)$. As we have seen in Sec. III A and Fig. 3, the samples investigated in this work have high values of δ, therefore we are going to consider the simplified equations with $\delta \approx 1$ as a good approximation for determining the degree of in-plane orientation of YBCO coated conductors with a high degree of *c*-axis grain fraction.

The angular dependence of the Raman intensity $I(\varphi)$ scattered from a coated conductor sample is dependent on the grain misorientation distribution present in the particular sample. The rotation angle φ, is defined as the angle between a sample edge and the polarization direction of the incident laser light. For the angular dependence of the Raman intensity of a particular phonon mode, we can write the equation

$$I(\varphi) = \sum_{i=0}^{n} P_i(\theta_i) I(\varphi + \theta_i), \tag{6}$$

where $P_i(\theta_i)$ is defined as the fraction of crystals with a misorientation angle θ_i according to some angle distribution function, and $I(\varphi+\theta_i)$ is its Raman intensity angular φ dependence.

From Eq. (6) we derived the expressions for the intensity dependence on the rotation angle of the depolarized spectra for the O(2,3) mode, see Eq. (7):

$$\begin{aligned} I^d_{B_{1g}}(\varphi) = {} & 4\delta x^2_{B_{1g}} \\ & \times \left\{ A - 8\int_{-\pi}^{+\pi} P(\theta)\sin^2\theta\cos^2\theta d\theta \right\} \\ & \times \sin^2\varphi\cos^2\varphi + 4\delta x^2_{B_{1g}}\int_{-\pi}^{+\pi} P(\theta) \\ & \times \sin^2\theta\cos^2\theta d\theta, \end{aligned} \tag{7}$$

where A is the total grain population, verifying

$$A = \int_{-\pi}^{+\pi} P(\theta) d\theta. \tag{8}$$

According to Eq. (7), the scattered intensity has a term k_1 oscillating in φ like $\sin^2\varphi\cos^2\varphi$, and a φ-independent k_2 term

$$k_1 = 4\delta x^2_{B_{1g}} \left\{ A - 8\int_{-\pi}^{+\pi} P(\theta)\sin^2\theta\cos^2\theta d\theta \right\}. \tag{9a}$$

and

$$k_2 = 4\delta x^2_{B_{1g}} \int_{-\pi}^{+\pi} P(\theta)\sin^2\theta\cos^2\theta d\theta \tag{9b}$$

and therefore,

$$I^d_{B_{1g}}(\varphi) = k_1 \sin^2\varphi\cos^2\varphi + k_2. \tag{9c}$$

The magnitude of the term oscillating in φ is a direct measure of the degree of texture in a given sample. We can define a texture parameter Q_c as the coefficient of the term oscillating in φ in a given sample normalized to the same coefficient for a perfectly epitaxial oriented film ($k_1 = 4A\delta x^2_{B_{1g}}$):

$$Q_c = \frac{k_1}{4A\delta x^2_{B_{1g}}} = \frac{k_1}{k_1 + 8k_2} = \frac{\frac{k_1}{k_2}}{\frac{k_1}{k_2} + 8}. \tag{10}$$

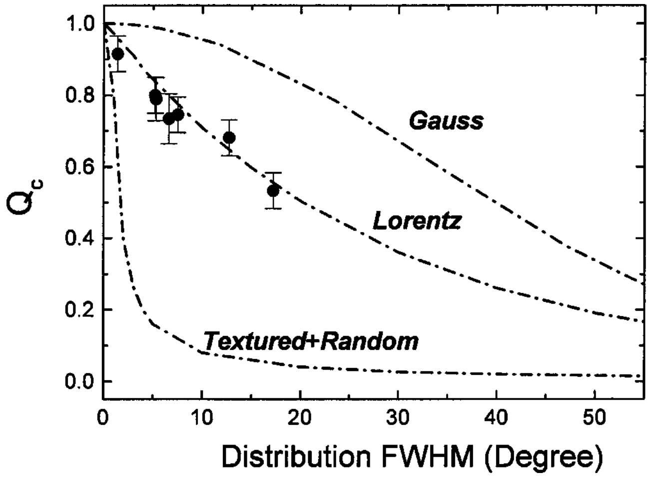

FIG. 5. Theoretical dependence of the texture parameter Q_c as a function of the FWHM of three different grain orientation distribution functions. Dots are the experimental Q_c values determined from micro-Raman measurements using Eq. (10) for all the samples analyzed as a function of the FWHM ϕ-scan (102) x-ray diffraction reflection.

A highly textured sample will be characterized by values of the Q_c parameter close to unity. On the contrary, poorly textured samples will have Q_c values close to zero.

The same treatment can be applied to analyze the angular dependence of the Raman intensity of the O(2,3) mode measured in polarized scattering configuration. The equation that describes the intensity modulation in this case is

$$\begin{aligned} I^p_{B_{1g}}(\varphi) = {} & \delta x^2_{B_{1g}} \left\{ A - 8\int_{-\pi}^{+\pi} P(\theta)\sin^2\theta\cos^2\theta d\theta \right\} \\ & \times (\sin^2\varphi - \cos^2\varphi)^2 \\ & + 4\delta x^2_{B_{1g}} \int_{-\pi}^{+\pi} P(\theta)\sin^2\theta\cos^2\theta d\theta \end{aligned} \tag{11a}$$

or,

$$I^p_{B_{1g}}(\varphi) = \tfrac{1}{4}k_1(\sin^2\varphi - \cos^2\varphi)^2 + k_2. \tag{11b}$$

This formulation enables us to assume different distribution functions, $P(\theta)$, in order to further analyze the material and thus provide information on the grain orientation distribution function present in a particular sample. A given distribution function reflects the abundance of different grain orientations in the film plane. We have calculated the theoretical dependence of the texture parameter, Q_c, as a function of the FWHM of three grain orientation distribution functions. In the most simple approximation, we considered that the films consist of a perfectly oriented and a randomly oriented parts (a simple 1 or 0 model). The intensity of the signal scattered from the perfectly oriented fraction is dependent of the rotation angle φ, and the intensity scattered from the randomly oriented fraction is φ independent. We have taken the value of the maximum of a normalized Gaussian function as the magnitude of the perfectly oriented part. As it can be seen in Fig. 5, the Q_c parameter value decays very

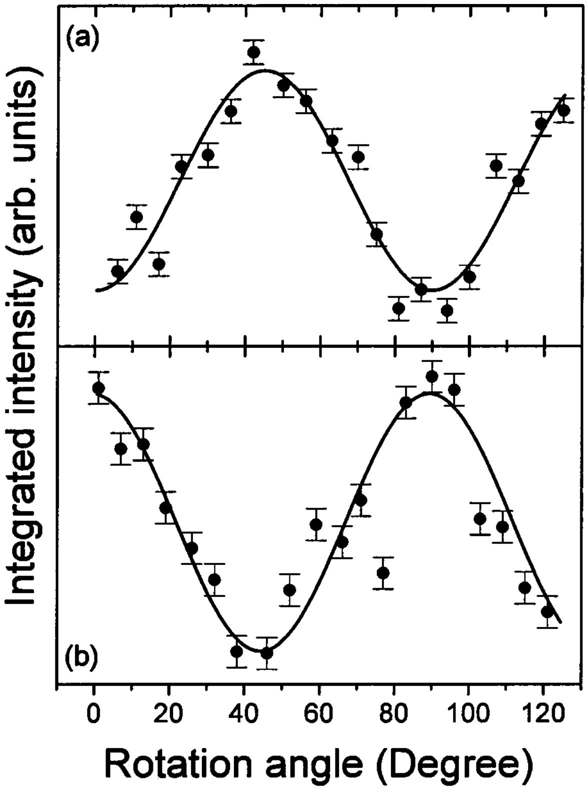

FIG. 6. Angular dependence of the integrated Raman intensity of the O$(2,3)$-B_{1g} Raman mode in IBAD-b sample measured in the depolarized geometry (a), and in the polarized geometry (b). The lines are the best fit values with δ=0.92, and Q_c=0.68±0.05.

fast to values close to zero. A similar model was previously assumed in Raman studies[11,12] analyzing the biaxial texture of YBCO films.

In order to formulate a more realistic view of the coated conductor samples, a Gaussian and a Lorentzian distribution of the grain orientation have instead been considered with the appropriate normalizations of Eq. (8). Figure 5 shows that the decay of the texture parameter Q_c with increasing FWHM of the distribution is moderate for the Lorentzian grain distribution and it goes to zero at an slower rate for a Gaussian grain distribution. It is clear from this theoretical study that the underlaying physics of the material will be determined by the particular distribution of the misoriented grains, and therefore these results validate the importance of modeling the Raman scattered intensities by using distribution functions.

From the experimental point of view, the intensity modulation were verified by rotating the sample from $\varphi=0°$ to $\varphi=120°$ and measuring the corresponding polarized and depolarized Raman spectra every 6°. The samples were mounted on a rotational microscope table whose perpendicular axis was carefully aligned with the optical axis of the microscope, so that always the same spot of the film remained in the focus during rotation. In Fig. 6, we show the angular modulation of the integrated Raman intensity of the O$(2,3)$ phonon mode measured in the depolarized scattering geometry for one representative sample, IBAD-b.

We fitted the angular dependence of the Raman intensity of the O$(2,3)$-B_{1g} mode measured in the depolarized scattering configuration using Eq. (9c). The values of k_1 and k_2 are determined from the numerical fit to the experimental Raman data. Q_c can be directly calculated using Eq. (10) from the value of k_1/k_2 evaluated from the fit to the experimental data. Expressing Q_c as a function of the k_1/k_2 ratio has the advantage to eliminate contributions of the particular detection system efficiency, the actual values of the Raman tensor elements, integration time, etc.

The experimental values of the angular dependence of the integrated Raman intensity of the O$(2,3)$-B_{1g} mode in the depolarized geometry for IBAD-b sample are displayed in Fig. 6(a). Also shown is the corresponding best fit function according to Eq. (9c). The value of Q_c obtained for this particular case when applying Eq. (10) is $Q_c=0.68\pm0.05$. For samples with $\delta>0.9$, that is the case for all the samples analyzed in this work, the Q_c values estimated from Eq. (10) differ in less than a 3% from those determined considering the *c*- and *a*-axis crystal population.

We have confirmed that the value of Q_c obtained from the fit to the depolarized configuration, also fits the angular dependence of the Raman intensity of the O$(2,3)$ mode when measured in the polarized scattering configuration. We show in Fig. 6(b), the experimental angular Raman intensity oscillations of the O$(2,3)$ phonon mode measured in polarized scattering geometry for the IBAD-b sample together with the calculated intensity oscillation using Eq. (11b) and the parameter values encountered in Fig. 6(a). Notice that a good agreement is obtained between theory and experiment. Similar agreement is also obtained for the other samples. Therefore, we can conclude that in order to determine the Q_c parameter only the depolarized Raman spectra is required to be analyzed.

Figure 5 also displays the Q_c experimental values determined by using Eq. (10) as a function of the FWHM ϕ-scan (102) reflection for the *c*-crystal domain for all the samples analyzed. A relationship is obtained between the Q_c parameter determined by micro-Raman and the x-ray ϕ-scan data, indicating that indeed both parameters are quantitatively related to the degree of biaxial texture of YBCO- coated conductors. Furthermore, it can be seen that an extremely good agreement with the experimental Raman results is obtained when using the Lorentz distribution function in our model. We conclude then, that micro-Raman is an interesting technique to investigate the grain orientation distribution function of coated conductors.

Moreover, the exponential decay of J_c with in-plane texture presented in Fig. 1 can now be described by the Q_c texture parameter, as shown in Fig 7. This figure shows the direct relationship existing between the Q_c parameter value calculated from the micro-Raman measurements in different kind of coated conductors and the critical current densities J_c. Micro-Raman scattering appears then as a technique to also investigate the superconducting properties of coated conductors.

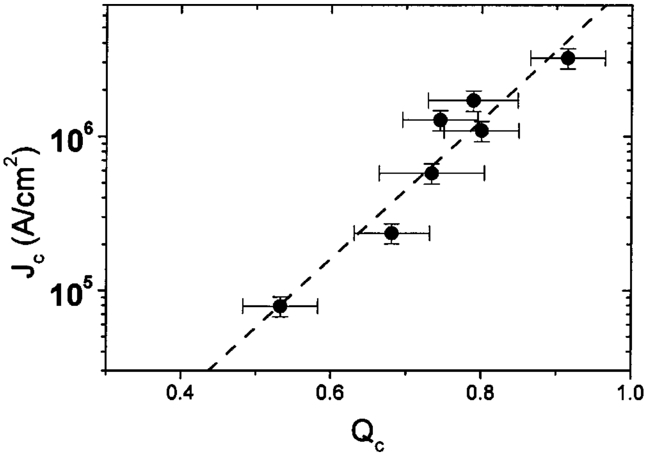

FIG. 7. Critical current densities, J_c; at 77 K as a function of the texture parameter Q_c, determined from micro-Raman measurements using Eq. (10) for all the different coated conductors investigated in this work.

D. Local evalution of biaxial texture

We have next evaluated the feasibility of micro-Raman to determine the uniformity of the in-plane texture of coated conductors. We have used the model described in the previous section to estimate Q_c at different points of samples with a high fraction of c-axis growth. We further simplified the experimental procedure to end up with a practical method to evaluate the local biaxial texture of YBCO-coated conductors. We determined the intensity oscillations only by measuring the depolarized scattering configuration of the O(2,3)-B_{1g} Raman mode at angle steps of 45° between 0° and 135° in order to minimize the measuring and evaluation times. This experimental simplification will enable us to determine the structure parameter Q_c in several sample positions in a reasonable time scale.

Figure 8 shows the experimental values of the angular intensity dependence of the depolarized O(2,3)-B_{1g} Raman mode and the corresponding best fit function according to Eq. (9c) for the IBAD-a sample. The Q_c value estimated for this particular sample and position according to Eq. (10) is $Q_c=0.77\pm0.05$, which is within the error bar of the value extracted from the full oscillation analysis shown in Fig. 5 ($Q_c=0.75\pm0.05$). This justifies the reduction of the experimental measurements down to four φ values for the determination of Q_c.

The first attempts to evaluate the uniformity of the degree of in-plane texture using the simplified model just described are presented in Fig. 9 for the IBAD-a sample. These results confirm that the in-plane texture of this particular sample is uniform, within our experimental accuracy, over large regions of the YBCO conductor.

In view of these results, we conclude that micro-Raman scattering is a powerful technique to evaluate the uniformity of the c-axis grain fraction and in-plane texture of coated conductors, and hence, of the uniformity of the critical current which we have demonstrated to be directly related to the degree of in-plane texture. Moreover, we have shown that a simplified modification of the model and the experimental procedure presented in this section enables to tackle this investigation with a reasonable time investment.

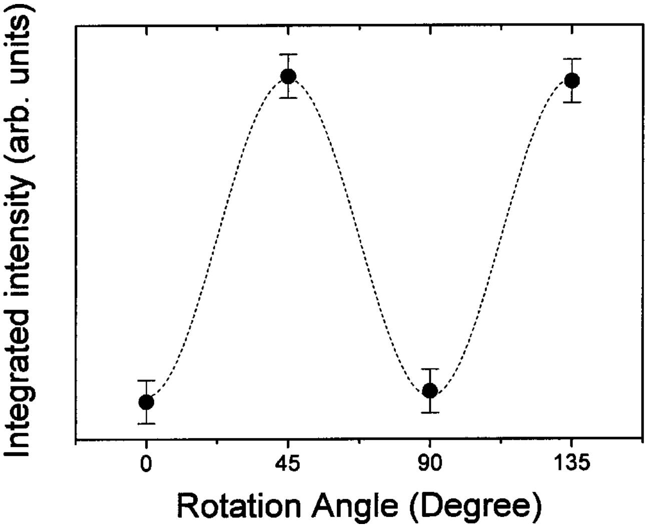

FIG. 8. Experimental values of the angular intensity dependence of the depolarized O(2,3)-B_{1g} Raman mode and the corresponding best fit function (dotted line) according to Eq. (9c) for the IBAD-a sample. The Q_c value obtained is 0.77 ± 0.05.

IV. CONCLUSIONS

We have demonstrated the high potentiality of micro-Raman spectroscopy for nondestructive biaxial texture analysis of YBCO-coated conductors. A simple methodology has been developed adapted to coated conductors based on the specific Raman selection rules for YBCO and polarized Raman scattering experiments. Detailed information on the epitaxial quality of the superconducting films is obtained from two parameters: c-axis oriented grains fraction, δ, and the degree of the in-plane orientation of the c crystals, Q_c. We have theoretically modeled the Raman scattering intensi-

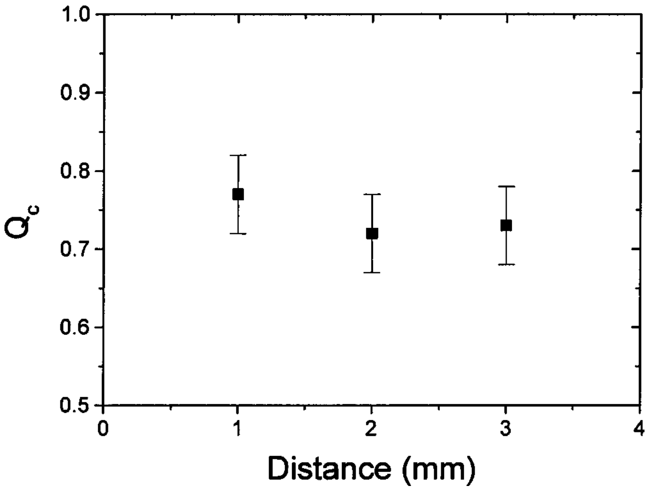

FIG. 9. In-plane texture, Q_c, of IBAD-a sample evaluated in three different points with a 10 μm laser spot according to the simplified model described in the text.

ties using different grain misorientation distribution functions and defining the Q_c parameter accordingly. The analysis of several samples with different in-plane orientation have proved that coated conductors are governed by a Lorentz distribution. We have confirmed, therefore, that Q_c is a true parameter to extract the degree of in-plane texture and grain misorientation distribution of YBCO coated conductors. The feasibility and uniqueness possibility of micro-Raman to study the biaxial texture sample uniformity has been demonstrated for coated conductors and a simplification of the model developed has been presented in this case.

ACKNOWLEDGMENTS

This work has been supported by MCYT (MAT2002-02642), Generalitat de Catalunya (SGR 2001-00189 and CeRMAE) and EU (SOLSULET G5RD-CT2001-00550). Financial support from AECI is acknowledged.

[1] D. Larbalestier, A. Gurevich, D. Mathew, and A. Polyanskii, Nature (London) **414**, 368 (2001).

[2] D. M. Feldmann, J. L. Reeves, A. Polyanskii, G. Kozlowski, R. R. Biggers, R. M. Nekkanti, I. Maartense, M. Tomsic, P. Barnes, C. E. Oberly, T. L. Peterson, S. E. Babcock, and D. C. Larbalestier, Appl. Phys. Lett. **77**, 2906 (2000).

[3] D. T. Verebeyi, D. K. Christen, R. Feenstra, C. Cantoni, A. Goyal, D. F. Lee, P. N. Arendt, D. F. DePaula, J. R. Groves, and C. Prouteau, Appl. Phys. Lett. **76**, 1755 (2000).

[4] C. Y. Yang, S. E. Babcock, A. Ichinose, A. Goyal, D. M. Kroeger, D. F. Lee, F. A. Lis, D. P. Norton, J. E. Mathis, M. Paranthaman, and C. Park, Physica C **377**, 333 (2002).

[5] A. Goyal, S. X. Ren, E. D. Specht, D. M. Kroeger, R. Feenstra, D. Norton, M. Paranthaman, D. F. Lee, and D. K. Christen, Micron **30**, 463 (1999); L. Fernández, B. Holzapfel, F. Schindler, B. de Boer, A. Attenberger, J. Hänisch, and L. Schultz, Phys. Rev. B **67**, 052503 (2003).

[6] S. R. Foltyn, P. N. Arendt, P. C. Dowden, R. F. DePaula, J. R. Groves, J. Y. Coulter, Q. Jia, M. P. Maley, and D. E. Peterson, IEEE Trans. Appl. Supercond. **9**, 1519 (1999); Ch. Joos, L. O. Kautschor, M. P. Delmamare, B. Bringmann, K. Guth, V. Born, S. Sievers, H. Walter, J. Dizk, J. Hoffmann, H. C. Freyhardrt, B. De Boer, B. Holzapfel, and F. Sandiumenge, Mater. Res. Soc. Symp. Proc. **659**, 117.1.1 (2001).

[7] L. A. Farrow, T. Venkatesan, W. A. Bonner, X. D. Wu, A. Inam, and M. S. Hegde, J. Appl. Phys. **65**, 4452 (1989).

[8] E. García-González, G. Wagner, M. Reedyk, and H.-U. Habermeier, J. Appl. Phys. **78**, 353 (1995).

[9] O. Martínez, J. Jiménez, D. Chambonnet, and C. Belouet, J. Mater. Res. **15**, 1069 (2000).

[10] U. Weimer, R. Freile, P. Leiderer, U. Poppe, J. Schubert, J. Fröhlingsdorf, B. Stritzker, and W. Zander, Physica C **168**, 359 (1990).

[11] C. Thomsen, R. Wegerer, H.-U. Habermeier, and M. Cardona, Solid State Commun. **83**, 199 (1992).

[12] N. Dieckmann, R. Kursten, M. Lohndorf, and A. Bock, Physica C **245**, 212 (1995).

[13] T. Puig, A. Puig-Molina, N. Mestres, H. Van Seijen, F. Alsina, J. C. González, X. Obradors, H. Graafsma, A. Usoskin, and H. C. Freyhardt, Mater. Res. Soc. Symp. Proc. **659**, II5.6.1 (2001).

[14] O. Castaño, A. Cavallaro, A. Palau, J. C. González, M. Rossell, T. Puig, F. Sandiumenge, N. Mestres, S. Piñol, A. Pomar, and X. Obradors, Supercond. Sci. Technol. **16**, 45 (2003).

[15] A. Usoskin, F. García-Moreno, S. Siever, J. Dzick, and H. C. Freyhardt, Inst. Phys. Conf. Ser. **167**, 447 (2000).

[16] R. Feenstra (unpublished).

[17] A. Palau, T. Puig, X. Obradors, A. Usoskin, H. C. Freyhardt, L. Fernández, and B. Holzapfel, IEEE Trans. Appl. Supercond. **13**, 2599 (2003).

[18] R. Liu, C. Thomsen, W. Kress, M. Cardona, B. Gegenheimer, F. W. de Wette, J. Prade, A. D. Kulkarni, and U. Schroeder, Phys. Rev. B **37**, 7971 (1988).

[19] C. Thomsen, in *Light Scattering in Solids VI*, Topics in Applied Physics, 68, edited by M. Cardona and G. Güntherodt (Springer, Berlin, 1991), p. 285.

[20] C. Hammond, *The Basics of Crystallography and Diffraction*, International Union of Crystallography Texts on Crystallography 5 (Oxford University Press, Oxford, 2001).

[21] J. Kircher, M. K. Kelly, S. Rashkeev, M. Alouani, D. Fuchs, and M. Cardona, Phys. Rev. B **44**, 217 (1991).